Magnetically Responsive Nanocomposite Hydrogels for Controlled Release of Ciprofloxacin

Abou El Fadl, Faten Ismail*[+•]

Prince Sattam Bin Abdulaziz University, Faculty of Science and Humanities, Hawtat Bani Tamim, SAUDI ARABIA

Maziad, Nabila

Polymer Chemistry Department, National Center for Radiation Research and Technology, Egyptian Atomic Energy Authority, Cairo, EGYPT

El Hamouly, Sabrnal; Hassan, Hassan El

Department of Chemistry, Faculty of Science, Minofia University, EGYPT

ABSTRACT: *Despite the huge work concerning the applicability of polymeric hydrogels in the field of drug release, it is still a promising and interesting area for more improvements and trials for preparing newly designed drug delivery systems. In this study, acrylamide and hydroxyl ethyl methacrylate (HEMA) copolymer hydrogels were prepared with the aid of gamma radiation, and the P(AAM/HEMA) nanocomposite hydrogels were obtained by in situ absorption and reduction method of iron salts and silver nitrates ($AgNO_3$) to form P(AAM/HEMA)-Fe_3O_4 and P(AAM/HEMA)-Ag nanocomposites. The prepared hydrogels and the formed nanoparticles were studied by various techniques; FT-IR, TEM, SEM, and the gel content and swelling behavior were evaluated. FT-IR confirmed the high interaction, which resulted in the successful formation of the AAm/HEMA copolymer hydrogel. TEM provides a good evaluation of the size of the formed Fe_3O_4 and Ag NPs to be 12 and 8.5 nm respectively. The prepared hydrogels and nanocomposite hydrogels were examined as drug delivery systems for Ciprofloxacin HCl as a model drug. The results showed that PAM/HEMA-Fe_3O_4 nanocomposite gave the suitable load and release behavior towards Ciprofloxacin HCl.*

KEYWORDS: *Acrylamide; Swelling and gel fraction; Ciprofloxacin; Gamma radiation; Drug loading, and release.*

INTRODUCTION

Metal nanoparticles embedded hydrogels have attracted attention these days mainly due to their wide range of applications in the field of catalysis, biomedicine, optics, pharmaceuticals, etc.[1]. A variety of copolymer hydrogel matrices based on various synthetic polymers, like polyvinyl alcohol (PVA), polyvinyl pyrolidone (PVP), etc., have been developed.

Among the different metal nanoparticles, most of the studies have been performed with noble metals, like silver and gold. But, to avoid the synthetic routes for the creation of metal nanoparticles following chemical reduction methods, which cause toxicity and biological hazards, developing new approaches, to incorporate metal nanoparticles into polymeric hydrogel matrices, as radiation technique is preferred [2,3]. Radiation technology is one such method, by which it is possible to synthesize nanoparticles, in situ in the hydrogel matrix. The properties of these nanomaterials are meaningfully changing by increasing the surface-to-volume ratio.

* *To whom correspondence should be addressed.*
+ *E-mail: fatenelramly555@yahoo.com*
• *Other Address: Polymer Chemistry Department, National Center for Radiation Research and Technology, Egyptian Atomic Energy Authority, Cairo, EGYPT*
1021-9986/2022/9/2873-2885 13/$/6.03

Stimuli-responsive polymers, which can respond to many factors, such as pH, temperature, and electric field, have attracted excessive attention due to their extensive applications in the field of controlled drug delivery. Polymeric hydrogel nanocomposites are a mixture of polymers with inorganic and organic additives with spherical structures dispersed through the polymer network structure [4]. Nanocomposites via polymeric matrix are often prepared by one of the extant synthetic routes such as melt-processing, sol-gel methods, and in situ polymerization, where in the case of the last two methods radiation technique can be used successfully without the need to add additional materials as crosslinkers and/or initiators which is suitable for the application in the biomedical field. Significant progress has been accomplished in the development of magnetic hydrogels (e.g., γ -Fe_2O_3, Fe_3O_4, Co Fe_2 O_4 nanocomposite hydrogels) that can quickly respond to an external magnetic field, allowing their improved controllability[5]. Here, we stress hydrogels containing Magnetic NanoParticles (MNPs) that have been recognized to be more appropriate than those with micron-sized particles for biomedical applications, due to their super-paramagnetic and responsive properties[6, 7].

Due to health-related dysfunctions, drug delivery targeting the site at therapeutic levels for a prolonged period is a major objective. However, the action of the pharmaceutical agent is confined by several factors including drug degradation, interaction with cells, and inability to infiltrate tissues. These factors provide the basis for developing carrier systems with the desired release profile with regard to time and drug distribution[8].

A drug-delivery system must be able to control solute release over time; thus, the development of drug-delivery systems requires the control of the water content within the polymeric structure. This is one of the most important factors influencing solute transport. In the last few years, various materials have been used for this purpose; however, hydrogels show two distinct advantages. First, drugs can easily diffuse through the hydrogels. The permeation rate can be controlled either by changing the crosslinking densities or by preparing the hydrogel with monomers of controlled hydrophilicity. Second, hydrogels may interact less strongly with the drugs than more hydrophobic materials; consequently, a larger fraction of active molecules can leave the hydrogel [9].

There are many works related to the applicability of acrylamide hydrogels as drug carriers eg. *Shahid Bashir et al.* (2017) [10] prepared pH-responsive N-succinyl chitosan/Poly (acrylamide-co-acrylic acid) hydrogels and studied the in vitro release of 5-fluorouracil; *Cinthia J. Pe´rez-Martı´nez et al.* (2020) [11] prepared novel composite hydrogels of poly(acrylamide) (PAAm) and starch, at different ratios, and studied the potential platforms for controlled release of amoxicillin also, *Vijaya Kumar Naidu Boya et al*. (2019) reported the synthesis of new drug carrier poly (acrylamide-co diallyldimethylammoniumchloride) nano gels (PAD-NG) by dispersion polymerization technique. these nano gels as intracellular drug delivery vehicles gave encapsulating 5-fuorouracil (5-FU) efficiency of 76.34% [12].

The focus of this work is on radiation preparation of novel acrylamide/HEMA embedded with magnetite and silver nanoparticles and investigation on the physiochemical properties of this drug carrier as a new polymer to be used as a delivery device in a wide range of pH values and to study the drug release (Ciprofloxacin) in this medium. The preparation was carried out by using in situ absorption reduction method as a simple and easy method. AAM and HEMA were used in this study to measure their suitability as drug delivery matrix for the model drug Ciprofloxacin HCl. By keeping the potential application of both HEMA and PAAM in mind, we have tried to synthesize a crosslinked network polymer hydrogel using gamma radiation.

EXPERIMENTAL SECTION

Materials

HEMA (2-Hydroxyethyl methacrylate) 97% and Acrylamide (AAM) 98% were purchased from Alfa Aesar Germany. Iron (II) chloride tetrahydrate (99C %) ($FeCl_2.4H_2O$), iron (III) chloride hexahydrate (99C %) ($FeCl_3.6H_2O$), and $AgNO_3$ were purchased from Acros. Ammonium hydroxide (0.5 M) (25%) was purchased from ADWIC Co. Egypt) and used without further purification.

Preparation of P(AAM/HEMA) hydrogels

Firstly, different formulations of AAM/HEMA were prepared from 20% (wt/v) concentration of HEMA and 10% (wt/v) concentration of AM. After that, the mixtures were mixed with a magnetic stirrer for 30 min to form homogenous polymer solutions with various compositions (80/20, 70/30, 60/40, 50/50, 40/60, 30/70,

and 20/80 (AAM/HEMA)). Finally, the solution was filled into 150 mL beakers and subjected to gamma-irradiation up to 20 kGy using a ^{60}Co facility to prepare P(AAM/HEMA) Hydrogels. The obtained hydrogels were removed, washed with double distilled water, and dried in an oven at 50°C for 24 h.

Preparation of P(AAM/HEMA)-Fe_3O_4 magnetic nano-composites

The magnetic nano-composite hydrogel was prepared by placing P(AAM/HEMA) hydrogel sample with the ratio (70/30) (Previous section), in 50 mL of double distilled water and allowed it to swell completely over a period of 24 h. The hydrogel was then, transferred to another beaker containing 200 mL of water containing 5 g of $FeSO_4$ and 10 g of $FeCl_3$ completely dissolved, and left for 24 h to entrap the iron salts throughout the hydrogel network. Then the loaded hydrogel was removed from the solutions and then, soaked in doubled distilled water for another 24 h, in order to remove unbound iron ions from the hydrogel surface. Loaded hydrogels were transferred into 25% of Ammonium hydroxide solution for 5h[13] to enhance the co-precipitation of iron ions within the hydrogel matrix and form Fe_3O_4 NPs[14]. The obtained black-colored magnetic hydrogel was removed and washed with deionized water for another 12 h and then dried in an oven at 50°C for 24 h.

Preparation of P(AAM/HEMA)–Ag nanocomposites

The preparation of Silver nanoparticles loaded hydrogel was performed in the following steps; Dry P(AAM/HEMA) hydrogel with a composition ratio (70/30) (Section 2.2) was placed in 100 mL of 1 M of $AgNO_3$ Solution and allowed to swell silver ions solution for 24 h then washed with double distilled water. Then silver ions loaded hydrogels were transferred to another beaker containing 100 mL of 6 mM sodium borohydride solution, instantly the reduction took place strongly due to the reduction of Ag^+ ions to Ag nanoparticles (Ag NPs) and as a result, the color of the hydrogel turned deep brown.

Chart flow for the experimental steps of preparations

Gel Fraction

Hydrogel samples were immersed in deionized water for 2 h under heating to remove the sol part. After that, the samples dried at 50°C in a vacuum. The gel fraction was calculated using Equation 1[15]:

$$\text{Gel Fraction} = \left(\frac{G_d}{G_i}\right)x100 \quad (1)$$

Where G_i is the initial mass of the sample and G_d is the mass of dried gel after extraction.

Swelling studies

The dried P(AAM/HEMA) different hydrogels at different compositions were equilibrated in distilled water and buffer solutions at different pH values (2, 5, 7.4, and 9) until constant weight. The equilibrium swelling capacity or swelling ratio (Q) of P(AAM/HEMA) Hydrogels were calculated by equation 2[16]:

$$Q = \left[\frac{m_t - m_o}{m_o}\right]x100 \quad (2)$$

Where m_t is the weight of the swollen gel at equilibrium and m_o is the weight of the dried gel[17].

The kinetic study for the prepared hydrogels was evaluated using the most used Fikian relation.

The following useful equation was used to determine the nature of the diffusion of water into hydrogels[18]:

$$Kt^n = \frac{M_t}{M_\infty} \quad (3)$$

Where M_t and M_∞ denote the amount of solvent diffused into the gel at time t and at the infinite time respectively, K is a constant related to the structure of the network and n is a characteristic exponent of the transport mode of the solvent. To elucidate the transport mechanisms, the swelling curves were fitted to the following equation:

$$\text{Log}\frac{M_t}{M_\infty} = \text{Log K} + \text{n Log t} \quad (4)$$

Drug loading to the polymeric matrix

Samples of 1g of the different (70/30) P(AAM/HEMA), (70/30) P(AAM/HEMA)-Fe_3O_4, and (70/30) P(AAM/HEMA)-Ag gel samples immersed in an aqueous solution of ciprofloxacin drug, which was selected as a model drug for this study with a concentration range of (100, 250, 300, 500, and 700 mg/L) at 25 C. The swelling equilibrium method was used to encapsulate the model drug inside the tested various samples. First, the (70/30) P(AAM/HEMA), (70/30) P(AAM/HEMA)-Fe_3O_4, and (70/30) P(AAM/HEMA)-Ag gel samples were left

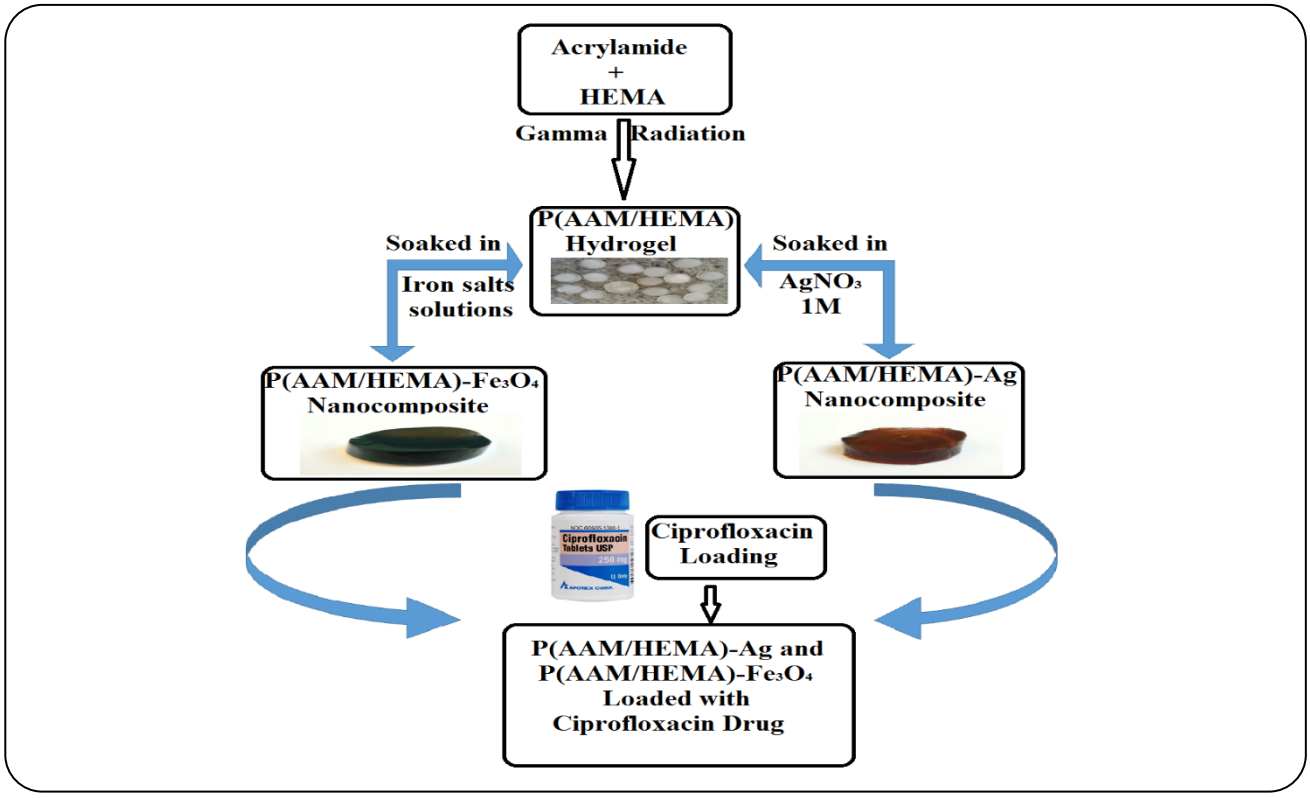

Fig. 1: Flowchart illustrates the preparation steps of hydrogels and nanocomposite hydrogels.

overnight in a 250 mg/L concentration of ciprofloxacin solution at room temperature. Subsequently, the swollen (70/30) P(AAM/HEMA), (70/30) P(AAM/HEMA)-Fe_3O_4, and (70/30) P(AAM/HEMA)-Ag gel samples loaded with ciprofloxacin dried in a vacuum oven at 50 ºC for 24 h. Drug-loaded hydrogels were put in 20 mL of various buffers at a wide range of pH for comparison (pH 2, 5, 7.4, and 9) for 24 h under vigorous stirring to extract the loaded drug from the hydrogels. The loading efficiency of the ciprofloxacin into the different (70/30) P(AAM/HEMA), (70/30) P(AAM/HEMA)-Fe_3O_4, and (70/30) P(AAM/HEMA)-Ag gel samples were determined by ultraviolet (UV)-Vis spectrophotometer at a fixed wavelength (λ_{max}= 275 nm). % of drug loading by different (70/30) P(AAM/HEMA), (70/30) P(AAM/HEMA)-Fe_3O_4, and (70/30) P(AAM/HEMA)-Ag gel samples selected based on the diffusional and swelling results were calculated by the following equations[19] (2):

$$\text{Loading of drug \%} = \left[\frac{M_D - M_o}{M_o}\right] \times 100 \qquad (5)$$

Where M_o is the initial weight of the hydrogel and M_D is the weight of the drug-loaded hydrogel[20].

Drug release measurements

Ciprofloxacin release designed at 25 ºC. Release experiments were conducted by placing the different (70/30) P(AAM/HEMA), (70/30) P(AAM/HEMA)-Fe_3O_4, and (70/30) P(AAM/HEMA)-Ag gel samples loaded with ciprofloxacin (conc.250 mg/L) into 20 mL buffer solutions of a wide range of pH (pH 2, 5, 7.4 and 9). The amount of drug released from (70/30) P(AAM/HEMA), (70/30) P(AAM/HEMA)-Fe_3O_4, and (70/30) P(AAM/HEMA)-Ag gel samples were calculated using the next Eq. (3) [21]:

$$\text{Drug release (\%)} = \left[\frac{M_o}{M_t} - 1\right] \times 100 \qquad (6)$$

Where M_t is the mass of the amount of drug released at time t and M_o is the initial mass of drug-loaded in the hydrogel[22].

Characterizations

IR Spectroscopy

The infrared spectra of the different copolymer hydrogels and their nanocomposites performed on a Mattson 5000 FT-IR spectrometer over the range of 200–4000 cm^{-1}.

Transmission Electron Microscopy

The size of the nano-particles in (70/30) P(AAM/HEMA)-Fe_3O_4, and (70/30) P(AAM/HEMA)-Ag network was determined using a Technai F12 TEM (Philips Electron Optics, Holland). The particle size of magnetic and Ag nanoparticles in TEM images was measured using NIH Image software (Mag D 20000x and HV D 80.0 kV).

X-ray Diffraction

X-Ray Diffraction (XRD) of (70/30) P(AAM/HEMA), (70/30) P(AAM/HEMA)-Fe_3O_4, and (70/30) P(AAM/HEMA)-Ag data were collected using Rigaku 2550D/max VB/PC X-ray diffractometer using Cu Kα radiation (λ = 1.54056Å).

UV- spectroscopy

A UV/VIS spectrometer model UV2 series made by Unicam, used at a wavelength range of 190–900 nm.

Magnetic Properties

Magnetic properties of pure Fe_3O_4, (70/30) (PAM/HEMA)-Fe_3O_4, and (70/30) PAM/HEMA/Ag gel were determined through VSM analyses Unit at Nanotechnology Characterization Center (NCC), Agriculture Research Center (ARC) Model: Lake Shore 7410.

RESULTS AND DISCUSSIONS

Gel fraction percent of P (AAM/HEMA) copolymer hydrogel

The gel content of copolymer hydrogels obtained from AAM/HEMA with different compositions (100/0, 90/10, 80/20, 60/40, 50/50, 40/60, 20/80, and 0/100 (AAM/HEMA)) prepared at a dose of 20 kGy were studied and illustrated in Fig. 2a. Studying the gel content of the prepared (PAM/HEMA) copolymer hydrogels revealed that the gel content decreased with increasing HEMA content in the AAM/HEMA copolymer hydrogels. Fig. 2a shows also, that increasing the HEMA content from 0% to 60 % the gel fraction decreased from 95% to only 94% but with a further increase in the HEMA content of more than 50% the Gel fraction decreased from 94% to 88%.

Based on the gel fraction results and handling reasons the P(AAM/HEMA) copolymer hydrogel with composition 70/30(AAM/HEMA) is chosen as the optimum condition and subjected to various radiation doses (20, 30, 40, 60, and 100 kGy) to study the variation of gel content and swelling properties due to the effect of radiation on the crosslinking density. As shown in Fig. 2b the Gel Fraction of pure HEMA is much higher than that of PAM and because of mixing HEMA with AAM, the Gel Fraction of the resultant copolymer hydrogel was lower than that of both PAM and PHEMA at various irradiation doses[23].

When the aqueous solution of AAM/HEMA is subjected to gamma irradiation, free radicals are generated and the random reactions of these radicals lead to the copolymerization of acrylamide and HEMA[24]. When the radiation dose increases beyond a certain value, the polymer chains crosslink, and then a gel-like material is obtained[25]. For the formation of crosslinked macromolecules, the subsistence of two radicals on neighboring chains and their subsequent combination are required[26].

Swelling Properties

Various factors that affect the equilibrium swelling of prepared P(AAM/HEMA) hydrogels were studied. Fig. 3 a and b illustrate the effect of P(AAM/HEMA) hydrogel various compositions and irradiation doses on the equilibrium swelling of 70/30 P(AAM/HEMA) composition compared with that of PAM (100%) and PHEMA (100%) hydrogels. It is noticed from Fig. 3a that as the HEMA content in the compositions increases the equilibrium swelling increase until reaching 30% of HEMA content in the resulting P(AAM/HEMA) hydrogel then starts to decrease from nearly 1600% at 30% content of HEMA to 200% at 80% content of HEMA. This may be attributed to the fact that with increasing the monomer content (HEMA) in the compositions the crosslinking density increases and as a result the equilibrium swelling decrease[27]. It is worth mentioning here that monomers differ in their ability to crosslink to form hydrogels under the effect of radiation due to differences in reactivity, functional groups, and reactivity[15]. Fig. 3b shows the effect of irradiation dose in the range from 20 up to 100 kGy on the equilibrium swelling of 70/30 P(AAM/HEMA) copolymer hydrogel in comparison with those of pure PAAM and PHEMA hydrogels. It is noticed from Fig. 3b that, with increasing irradiation dose, from 20 to 100 kGy the equilibrium swelling decreases for all samples. This again due to that increasing irradiation dose cause increase in the gel fraction and as a result the crosslinking density of the prepared copolymer hydrogel increased [28, 29].

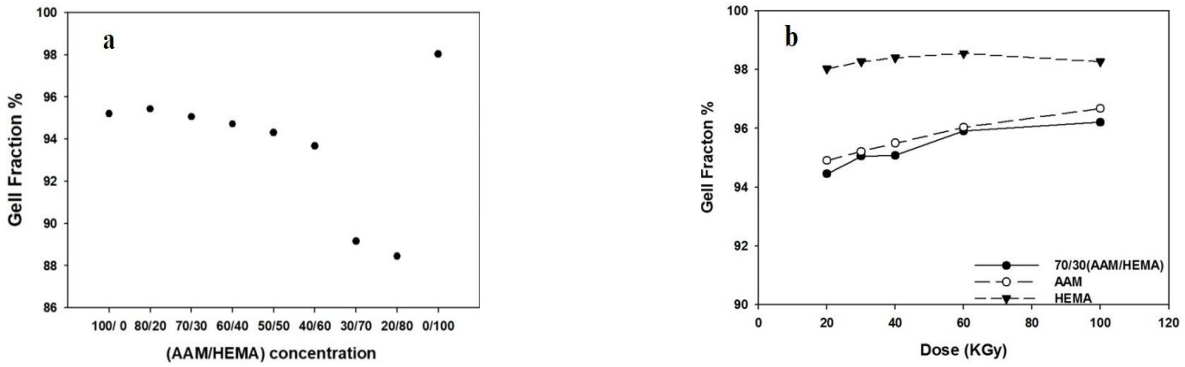

Fig. 2: Effect of HEMA monomer concentration on gel fraction percentage of P(AAM/HEMA) hydrogel at (20 kGy) (a) and Effect of different irradiation doses (kGy) on the gel fraction percent of prepared (○) (PAM) hydrogel, (▼) (PHEMA) hydrogel and (●) 70/30 P(AAM/HEMA) copolymer hydrogel (b).

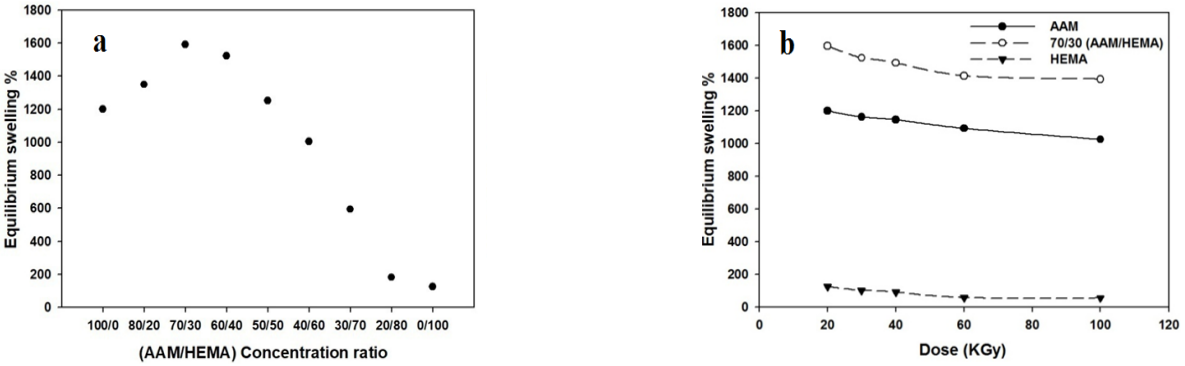

Fig. 3: a) Effect of HEMA monomer concentration on equilibrium swelling percentage of P(AAM/HEMA) hydrogel at (20 kGy), and b) Effect of different irradiation doses on equilibrium swelling percentage of (●) P(AAM), (▼) P(HEMA) and (○) P(AAM/HEMA) hydrogels.

Effect of pH on the equilibrium swelling of P(AAM/HEMA) hydrogel, P(AAM/HEMA)-Fe_3O_4 and P(AAM/HEMA)-Ag nanocomposites

pH is an important factor for the applicability of polymeric hydrogels as a drug delivery system. So, the swelling behavior of the prepared hydrogels and their nanocomposites with magnetite and Ag NPs examined and evaluated a broad range of pH values. Fig. 4 shows the equilibrium swelling of P(AAM/HEMA), P(AAM/HEMA)-Fe_3O_4, and P(AAM/HEMA)-Ag nanocomposites at various pH values. It is clear from this figure that the equilibrium swelling of P(AAM/HEMA)-Fe_3O_4 nanocomposite increases with increasing pH value up to pH5 and then started to decrease with a further increase in pH value of the medium. The Hydrogel P(AAM/HEMA) and the nanocomposites P(AAM/HEMA)-Fe_3O_4, and P(AAM/HEMA)-Ag swelled fairly slowly in the buffer solution and reached the equilibrium around 24 h depending on some parameters. Fig. 4 showed that the critical pH point for P(AAM/HEMA) hydrogel, P(AAM/HEMA)-Fe_3O_4, and P(AAM/HEMA)-Ag nanocomposites were 5, and it exhibits slight displacements based on acidic moiety content. The behavior of the P(AAM/HEMA) and P(AAM/HEMA)-Ag nanocomposites was also, illustrated in Fig. 4 where the equilibrium swelling slightly increases with increasing the pH value of the medium. The swelling capacity of a hydrogel is because of hydrophilic groups represented in the amid group provided by AAM that is entrapped inside the networks of P (AAM /HEMA) copolymer hydrogel. It was known that the polar

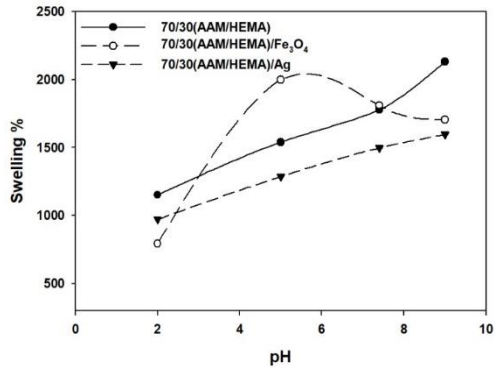

Fig. 4: Effect of pH on the Equilibrium swelling (●) 70/30(PAM/HEMA), (○) 70/30 (PAM /HEMA)/Fe_3O_4, (▼) 30/70(PAM/HEMA)/Ag at (20kGy).

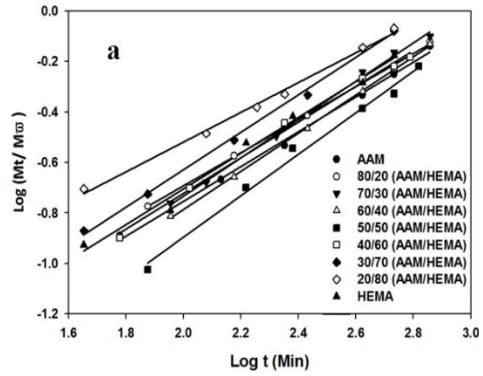

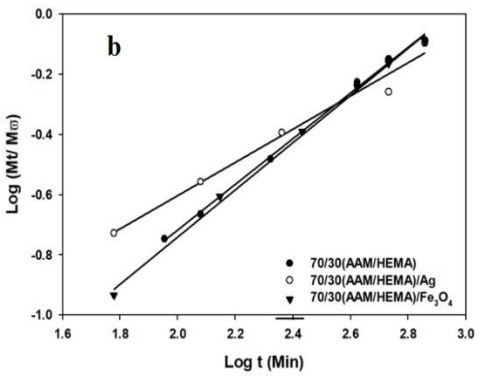

Fig. 5: a) Plots of log (M_t/M_∞) against log (t) for the (PAM/HEMA) copolymer hydrogel at different compositions, and b) Plots of log (M_t/M_∞) against log(t) for the 70/30 P(AAM/HEMA) copolymer hydrogel, 70/30 P(AAM/HEMA)-Ag, and 70/30 P(AAM/HEMA)-Fe_3O_4.

head groups of polymeric chains such as OH, NH_2, and $CONH_2$ have a high affinity for salts [30]**.** The equilibrium swelling results can be traced back to structural changes in the hydrogel matrix caused by nanoparticle integration. These results make the P(AAM/HEMA) copolymer hydrogel promising to be applied as a drug delivery system.

Fikian kinetics (Diffusion mechanism)

Fig. 5 a and b represent the Plots of log (M_t/M_∞) against log (t) for the P(AAM/HEMA) copolymer hydrogel at different compositions (Fig. 5a) and that of (PAM/HEMA)/Fe_3O_4, and (AAM/HEMA)/Ag nanocomposites, and the values of the exponents (n) are summarized in Table 1. Applying Equation 4 is possible only if the value of M_e is known. Thus, it could be used only for the samples that reached equilibrium swelling and exhibited a 'regular' character of swelling isotherm. From Fig. 5 a and b and Table 1, it is noticed that the diffusion behavior expressed in the values of the exponent (n) of P (AAM/HEMA) various compositions, (PAM/HEMA)/Fe_3O_4, and (AAM/HEMA)/Ag nanocomposites were more than 0.5. It is also, obviously noticed that the diffusion mechanism of the prepared P(AAM/HEMA) compositions, P(AAM/HEMA)/Fe_3O_4, and P(AAM/HEMA)/Ag nanocomposites follows non-Fickian diffusion in which the rate of diffusion is much more than that of relaxation which makes these hydrogels suitable as drug delivery system.

Characterization of P(AAM/HEMA) nanocomposites

Magnetic (Fe_3O_4) and silver (Ag NPs) nanoparticles are attracting attention because of their unique features [31,32]**.** The prepared hydrogel P(AAM/HEMA) was used to prepare P(AAM/HEMA)-Fe_3O_4, and P(AAM/HEMA)-Ag nanocomposites to be tested as drug delivery system for ciprofloxacin as a model drug. Photographic pictures of different P(AAM/HEMA**)** hydrogels before and after Fe_3O_4 and Ag NPs loading, respectively, and the mechanism of P(AAM/HEMA) copolymer formation by gamma radiation are shown in Fig. 6.

X-ray diffraction

The corresponding XRD patterns of P(AAM/HEMA) hydrogel, 70/30 P(AAM/HEMA)-Fe_3O_4, and 70/30 P(AAM/HEMA)-Ag, compared with pure Magnetite and pure Ag NPs are shown in Fig. 7. As shown in Fig. 7 P(AAM/HEMA) hydrogel have not exhibited any sharp

Table 1: Diffusion parameters of the P (AAM/HEMA) hydrogels with various compositions and its silver and magnetic nanocomposites.

P(AAM/HEMA) compositions	Nano Particles	N	Mechanism
100/0		0.69	Non-Fickian
70/30	-	0.76	Non-Fickian
0/100		0.71	Non-Fickian
70/30	Ag	0.55	Non-Fickian
70/30	Fe_3O_4	0.78	Non-Fickian

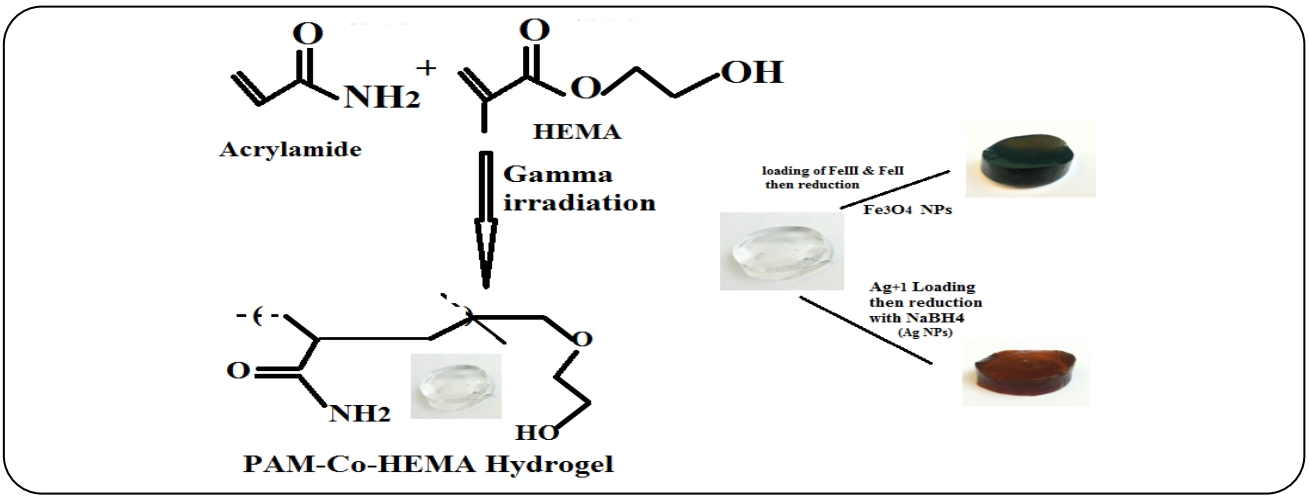

Fig. 6: Radiation preparation of P(AAM/HEMA) hydrogels and its magnetic and silver nanocomposites

peaks in XRD except for a broad peak around 2θ 25 which is due to the polymer network. The Fe_3O_4 nanocomposite hydrogel shows the diffraction peaks at about 35.03 (311), 43 (400), 58 (511), and 63(440) [33, 7] which are coincident with those for pure cubic Fe_3O_4 crystal diffraction peaks. The common diffraction peak for pure Fe_3O_4 has been observed at 2θ=35.03, 43, 58, and 63 with higher intensity than that in the case of 70/30 P(AAM/HEMA)-Fe_3O_4 nanocomposite, due to the amorphous nature of the prepared hydrogel. Silver nanocomposite hydrogel is characterized by XRD technique, as presented in Fig. 7 too. The P(AAM/HEMA)-Ag nanocomposite shows four prominent peaks at 2θ values of about 38◦, 43◦, 63◦, and 76◦ in agreement with the diffractogram of pure Ag NPs and the literature [34]. The hump at 2θ =20° is attributed to the amorphous nature of polymer hydrogel.

The size of the Ag NPs and Fe_3O_4 NPs estimated by using Scherer's formula:

$$\text{Crystallite average size } D = \frac{K\lambda}{\beta \cos\theta} \qquad (7)$$

Where D is the crystallite size in nm, λ is the radiation wavelength (0.154 nm for Cu K), β is the bandwidth at half-height and θ is the diffraction peak angle and k is a constant (0.9). The calculated crystallite average size was found to be 3.18, 4.8, 3.43, and 2.6 nm for 70/30 P(AAM/HEMA)-Fe_3O_4, 70/30 P(AAM/HEMA)-Ag, pure Magnetite and Ag NPs respectively.

Magnetic properties

In order to study the magnetic behavior of Fe_3O_4 nanoparticles and P(AAM/HEMA)-Fe_3O_4 magnetization measurements were performed. Typical magnetization curves for pure Fe_3O_4 and P(AAM/HEMA)-Fe_3O_4 are schematically represented in Fig. 8. As indicated in Fig. 8**,** the curve provides major characteristic parameters of magnetic materials: the saturation magnetization MS, the coercivity, and the remanence. The slope of the magnetization curve at H=0 gives the magnitude of the magnetic susceptibility. As can be seen from the figure the saturation magnetization of the P(AAM/HEMA)-Fe_3O_4 nanocomposite hydrogel was about 22.98 emu/g,

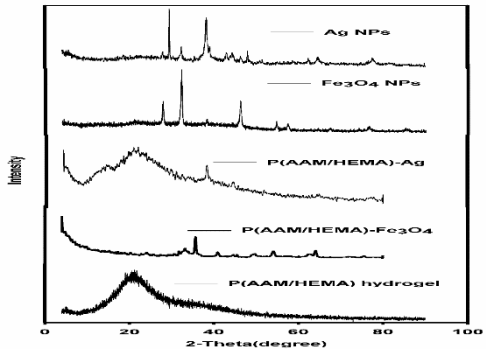

Fig. 7: XRD patterns of: 70/30 P(AAM/HEMA), 70/30 P(AAM/HEMA)-Fe_3O_4, 70/30 P(AAM/HEMA)-Ag, pure Magnetite and pure Ag NPs.

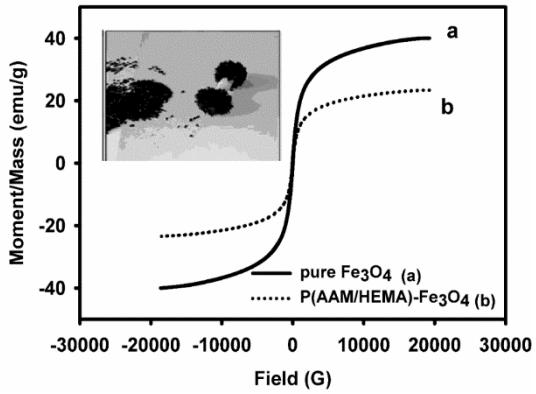

Fig. 8: (a) pure Magnetite Ms= 44.65 emu/g and (b) Magnetization saturation curve of P(AAM/HEMA)-Fe_3O_4 Ms= 22.98 emu/g.

which is lower than the reference value for the pure magnetite nanoparticles (44.65 emu/g) due to the effect of the polymer matrix[31]. As can be seen in Fig. 8, neither coercivity nor remanence was observed so the prepared P(AAM/HEMA)-Fe_3O_4 exhibited superparamagnetic behavior, a feature that is actually in accordance with what should be expected from their particle size.

Scanning Electron Microscopy

Changes in the morphology of the copolymer hydrogel prepared from AAM and HEMA mixture by the effect of gamma radiation P(AAM/HEMA) before and after incorporation of Fe_3O_4 MNPs and Ag NPs within the polymer matrix were studied using SEM technique. Fig. 9 (a, b, and c) shows the SEM surface morphology micrographs of P(AAM/HEMA) copolymer hydrogel, P(AAM/HEMA)/Fe_3O_4, and P(AAM/HEMA)/Ag nanocomposite hydrogel. The Surface morphology of P(AAM/HEMA) was found to be very smooth, homogeneous, and continuous with few cracks and discontinuities (Fig. 9 a), however, after the incorporation of Fe_3O_4 MNPs within parental P(AAM/HEMA) hydrogel copolymer a complete change in the morphology was observed. as shown in Fig. 9 b The surface converted into heterogeneous and fibrillar due to irregularities introduced by Fe_3O_4 magnetic nanoparticles. On the other hand, the incorporation of Ag NPs within P(AAM/HEMA) copolymer hydrogel better matrix coherence was achieved, and the heterogeneous and rough surface of the hydrogel matrix became more coherent and near co-continuous in the case of P(AAM/HEMA)/Ag nanocomposite hydrogel (Fig. 9 c). Moreover, successful incorporation and uniform distribution of Ag NPs within the hydrogel matrix was achieved and also confirmed by TEM.

Transmission Electron Microscopy (TEM)

Typical TEM images of P(AAM/HEMA)-Fe_3O_4, and P(AAM/HEMA)-Ag nanocomposite hydrogels are shown in Fig. 10 (a and b). Well-shaped spherical magnetic nanoparticles were observed in the TEM image of P(AAM/HEMA)-Fe_3O_4 nanocomposite hydrogel which confirmed that Fe_3O_4 NPs got incorporated homogeneously in the polymer matrix of P(AAM/HEMA) copolymer hydrogel **(Fig. 10 a)** and there is no aggregation is observed. The mean diameter of coated nanoparticles Fe_3O_4 as detected from TEM was nearly 12 nm. On the other hand, silver nanoparticles were observed in TEM image of P(AAM/HEMA)-Ag nanocomposite hydrogel (Fig. 10b). Silver nanoparticles size as detected from TEM was nearly 8.5 nm. This is nearly in accordance with the values obtained by using Scherer's equation.

Ciprofloxacin drug loading

Fig. 11 a and b illustrate the change in the loading percent with time and also, the effect of the initial concentration of the drug on the amount loaded (mg/g) by P(AAM/HEMA) copolymer hydrogels and their magnetic and silver nanocomposite hydrogels counterparts**.** The loading of Ciprofloxacin was monitored with time from a feed solution of 250 ppm of the drug as shown in Fig. 11 a and b. From this figure, it is noticed that the highest amount of loaded drug was for the magnetic nanocomposite hydrogel which was 220 mg/g after nearly 7h

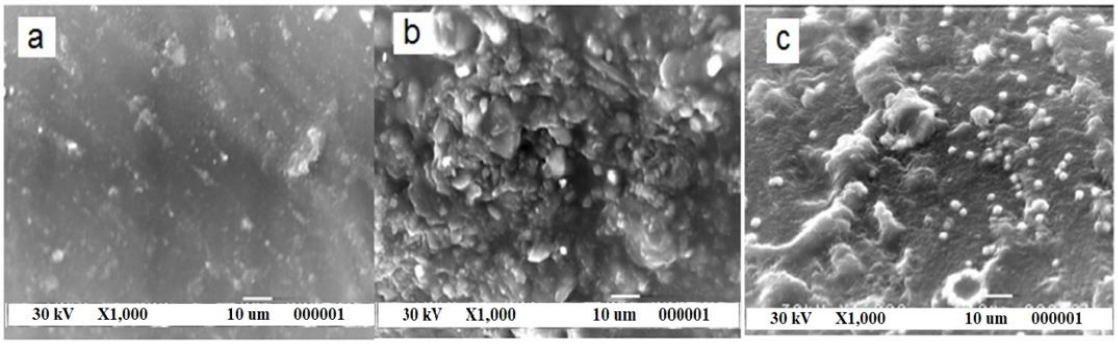

Fig. 9: a) SEM micrograph of (PAM/HEMA) hydrogel b) SEM micrograph of (PAM/HEMA)/Fe_3O_4 and c) SEM micrograph of (PAM/HEMA)/Fe_3O_4/Ag nanocomposite hydrogel.

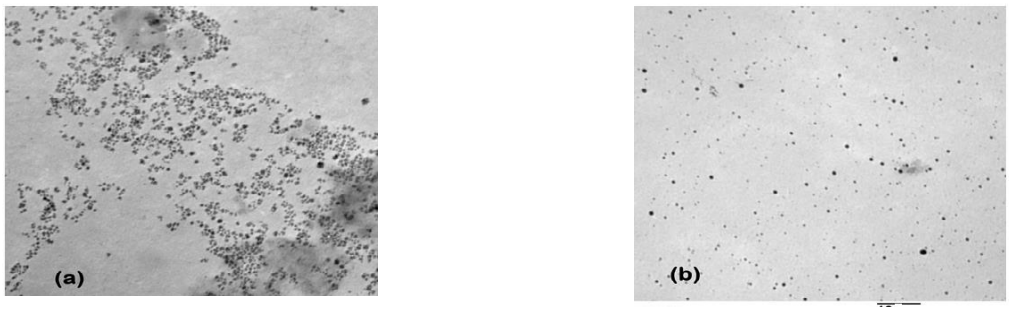

Fig. 10: TEM images of a) (P(AAM/HEMA)-Fe_3O_4, and b) P(AAM/HEMA)-Ag nanocomposite hydrogels (Mag=20000x and HV=80.0 kv).

while the amounts loaded by P(AAM/HEMA) hydrogel and P(AAM/HEMA)-Ag copolymer nanocomposite hydrogels were 101 and 130 mg/g respectively after 7h. On the other hand, studying the effect of various initial concentrations of Ciprofloxacin on its loading by P(AAM/HEMA), P(AAM/HEMA)-Fe_3O_4 and P(AAM/HEMA)-Ag copolymer nanocomposite hydrogels is another way to understand the behavior of prepared hydrogels and their nanocomposites toward the loading of Ciprofloxacin. As shown in **Fig. 11 b,** P(AAM/HEMA), P(AAM/HEMA)-Fe_3O_4, and P(AAM/HEMA)-Ag samples provide great loading affinity toward the drug where the amount of loaded drug increases with increasing the initial drug concentration from 100ppm up to 700 ppm and the P(AAM/HEMA)-Fe_3O_4 nanocomposite still, provides the highest loading affinity toward Ciprofloxacin.

Ciprofloxacin Release

The release of Ciprofloxacin by P(AAM/HEMA) hydrogel, P(AAM/HEMA)-Fe_3O_4 P(AAM/HEMA)-Ag nanocomposite hydrogels was monitored at various values (2-9) with time and illustrated in Fig. 12. It is noticed that, with increasing pH value of the medium up to 5 as shown in Fig. 12, the amount released of Ciprofloxacin from P(AAM/HEMA)-Fe_3O_4 nanocomposite was the highest (nearly 200 mg/g) compared to P(AAM/HEMA)-Ag nanocomposite hydrogel (90 mg/g), and P(AAM/HEMA) hydrogel (65 mg/g) at pH 5. But with a further increase in the pH of the medium to 7.4 the amount released of Ciprofloxacin from P(AAM/HEMA)-Fe_3O_4 nanocomposite P(AAM/HEMA)-Ag nanocomposite hydrogel, and P(AAM/HEMA) hydrogel decreases nearly to 80, 50, and 45 mg/g respectively. At pH 9, the amount released of Ciprofloxacin is nearly the same as in the case of pH 7.4 for all nanocomposite hydrogels. It is concluded from these results that pH 5 is the most suitable pH for the Ciprofloxacin release may be attributed to the fact that the drug has high solubility at pH 4-5 whereas, at high pKa values (low pH), ciprofloxacin is more soluble since it is in the protonated form. It is almost insoluble in water and alcohol. At pH 4-5 it shows the highest solubility[5].

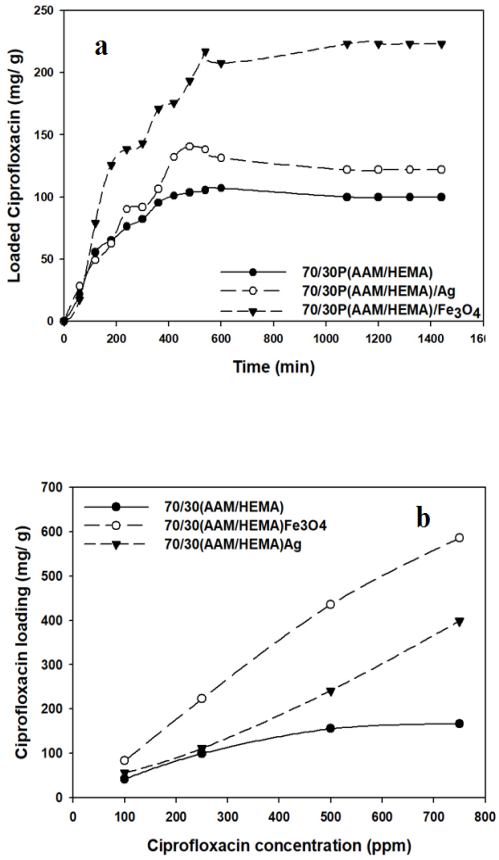

Fig. 11: a) Effect of time (min) on a load of Ciprofloxacin drug onto P(AAM/HEMA), P(AAM/HEMA)-Ag, and P(AAM/HEMA)-Fe_3O_4 hydrogels in distilled water. B) Effect of initial concentrations of Ciprofloxacin on its loading by P(AAM/HEMA), P (AAM/HEMA /HEMA)-Fe_3O_4 P(AAM/HEMA)-Ag nanocomposite hydrogels.

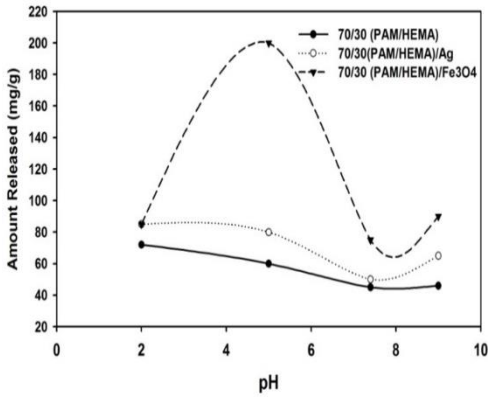

Fig. 12: Effect of pH on the release of Ciprofloxacin drug onto (AAM/HEMA), (AAM/HEMA)/Ag, and (AAM/HEMA)/ Fe_3O_4 hydrogels.

Ciprofloxacin is almost insoluble in the neutral pH range, while solubility increases with increasing pH value up to pH5. That is the reason behind studying the release behavior at a wide range of pH not only at pH 7.4. The obtained results of drug release also, are related to the structural and the formed network structure. lots of work done on acrylamide hydrogels as a drug delivery system as work done by L. *Ferreira et al*. (2001) [9]where their work based on studying the relation between swelling and diffusional properties on the Aspirin release by acrylamide hydrogels and they found that the observations of equilibrium swelling, solute transport, and thermal analysis are related to the network structure of polyacrylamide hydrogel.

CONCLUSIONS

The P(AAM/HEMA) and its magnetic and silver nanocomposites were successfully prepared. Studying the gel fraction and the swelling behavior concluded that the compositions (70/30) and (80/20) P (AAM/ HEMA) have the highest swelling affinity. TEM and XRD studies proved the formation of Fe_3O_4 and Ag particles in the nanoscale. The composition (70/30) P (AAM/ HEMA) was used for loading both Fe_3O_4 and Ag NPs and examined for the absorption and release of Ciprofloxacin as a model drug. The results revealed that with increasing the initial concentration of the drug the amount absorbed increases. Also, as a result, the amount of released drug increases with increasing the initial drug concentration. It is concluded also that the highest amount loaded and released from Ciprofloxacin was for the P(AAM/HEMA)-Fe_3O_4 nanocomposite. Polymer hydrogels with their unique properties open many channels and widen the applicability of the hydrogels in the drug delivery field. So authors can do further research on the nanocomposites of various polymer hydrogels using gamma radiation as a unique tool. Also, This experiment includes concepts like polymerization, crosslink density, magnetic nanocomposite hydrogel, and controlled release, topics which should be emphasized to students in the areas of chemistry, pharmacy and materials science. These concepts are also valuable for students with interests in the field of nanotechnology.

Received : Apr. 4, 2021 ; Accepted : Nov. 1, 2021

REFERENCES

[1] Ghasemzadeh H., Ghanaat F., Antimicrobial Alginate/PVA Silver Nanocomposite Hydrogel, Synthesis and Characterization, *J. Polym. Res.,* **21** (2014).

[2] Zhou Y., Zhao Y., Wang L., Xu L., Zhai M., Wei S., Radiation Synthesis and Characterization of Nanosilver/Gelatin/Carboxymethyl Chitosan Hydrogel, *Radiat Phys Chem* ., **81**: 553–560 (2012).

[3] Juby K.A., Dwivedi C., Kumar M., Kota S. Misra H. S., P N Bajaj P. N., Silver Nanoparticle-Loaded PVA/Gum Acacia Hydrogel: Synthesis, Characterization and Antibacterial Study, *Carbohydr Polym.*, **89**:906–913 (2012).

[4] Deen G., Chua V., Synthesis and Properties of New "Stimuli" Responsive Nanocomposite Hydrogels Containing Silver Nanoparticles, *Gels*, **1**: 117–134 (2015).

[5] Abou El Fadl F.I., Maziad N.A., El-Hamouly S.H., Hassan H.R., Synthesis and Characterizations of Various Polyvinyl Pyrrolidone/Hydroxyl Ethyl Methacrylate Nanocomposite Hydrogels as Drug Delivery Systems, *J. Macromol Sci Part A Pure Appl Chem.,* **55**:107–115 (2018).

[6] Dai Q.Q., Ren J.L., Peng F., Chen X.F., Gao C.D., Sun R.C., Synthesis of Acylated Xylan-Based Magnetic Fe_3O_4 Hydrogels and their Application for H_2O_2 detection. Materials (Basel) 9 (2016).

[7] Raju A.N.P.K.M., Development of Guar Gum based Magnetic Nanocomposite Hydrogels for the Removal of Toxic Pb^{2+} Ions from the Polluted Water, *Int J Sci Res.,* **5**: 1588–1595 (2016).

[8] Rashid A., Ahmad M., Tulain U. R., Iqbal F. M., Fabrication and Evaluation of 2-hydroxyethyl Methacrylate-Co-Acrylic Acid Hydrogels for Sustained Nicorandil Delivery, *Trop J Pharm Res.,* **14**: 1121–1128 (2015).

[9] Ferreira L., Vidal M. M., Gil M. H., Design of a Drug-Delivery System Based On Polyacrylamide Hydrogels, *Evaluation of Structural Properties. Chem Educ.*, **6**: 100–103 (2001).

[10] Bashir S., Teo Y.Y., Naeem S., Ramesh S., Ramesh K., pH responsive N-Succinyl Chitosan/Poly (Acrylamide-co-acrylic acid) Hydrogels and in Vitro Release of 5-Fluorouracil, *PLoS One.*, **12**: 1–24 (2017).

[11] Torres-Figueroa A. V., Pérez-Martínez C. J., Castillo-Castro T. Del., Bolado-Martínez E., Corella-Madueño M.A.G., García-Alegría A.M., Lara-Ceniceros T.E., Armenta-Villegas L., Composite Hydrogel of Poly(acrylamide) and Starch as Potential System for Controlled Release of Amoxicillin and Inhibition of Bacterial Growth, *J Chem*. (2020).

[12] Sana S.S., Arla S.K., Badineni V., Boya V.K.N., Development of Poly (acrylamide-co-diallyldimethylammoniumchloride) Nanogels and Study of their Ability As Drug Delivery Devices, SN *Appl Sci.,* **1**:1–10 (2019).

[13] Tanasa E., Zaharia C., Radu I. C., Surdu V. A., Vasile B.S., Damian C.M., Andronescu E., Novel Nanocomposites Based on Functionalized Magnetic Nanoparticles and Polyacrylamide: Preparation and Complex Characterization, *Nanomaterials*, **9(10)**: 1384 (2019).

[14] Baghban A., Jabbari M., Rahimpour E., Fe_3O_4@Polydopamine Core-Shell Nanocomposite as a Sorbent for Efficient Removal of Rhodamine B from Aqueous Solutions: Kinetic and Equilibrium Studies, *Iran. J. Chem. Chem. Eng. (IJCCE)*, **37**: 17–28 (2018).

[15] Mahmoud M.M., Abou El Fadl F.I., Mohamed M.A., Ibrahim S.M., Improvement of hydrophilicity of Natural Rubber Latex/Potato-Starch blend by grafting with Hydrophilic Monomers, *Iran Polym J.*, (2021).

[16] Asadi S., Eris S., Azizian S., Alginate-Based Hydrogel Beads as a Biocompatible and Efficient Adsorbent for Dye Removal from Aqueous Solutions, *ACS Omega.*, **3**: 15140−15148 (2018)

[17] Sabnam T., Monir B., Afroz S., Khan R.A., Miah M.Y., Takafuji M., Alam M. A., pH-Sensitive Hydrogel from Polyethylene Oxide and Acrylic Acid by Gamma Radiation, *J. Compos. Sci.*, **3**: 58 (2019)

[18] Ibrayeva Z., Blagikh E., Kudaibergenov S., Introduction II Mechanical Properties of Composite Hydrogel Materials Based on Poly (Acrylamide) and Clay Minerals and their Potential Application for Cleaning of the Internal Surface of Pipes, *Advances in Engineering Mechanics and Materials.*, 001(2003).

[19] Ranathunge T.A., Karunaratne D.G.G.P., Rajapakse R.M.G., Watkins D.L., Doxorubicin Loaded Magnesium Oxide Nanoflakes as pH Dependent Carriers for Simultaneous Treatment of Cancer and Hypomagnesemia, *Nanomaterials*., **9** (2019).

[20] Keirouz A., Radacsi N., Ren Q., Dommann A., Beldi G., Maniura-Weber K., Rossi R. M., Fortunato G., Nylon-6/chitosan Core/Shell Antimicrobial Nanofibers for the Prevention of Mesh-Associated Surgical Site Infection, *J. Nanobiotechnology*., **18**: 1–17 (2020).

[21. Motaali S., Pashaeiasl M., Akbarzadeh A., Davaran S., Synthesis and Characterization of Smart N-Isopropylacrylamide-Based Magnetic Nanocomposites Containing Doxorubicin Anti-Cancer Drug, *Artif Cells, Nanomedicine Biotechnol.*, **45**: 560–567 (2017).

[22] Abd El-Hady M.M., El-Sayed Saeed S.E.S., Antibacterial Properties and pH Sensitive Swelling of Insitu Formed Silver-Curcumin Nanocomposite Based Chitosan Hydrogel, *Polymers*., (Basel) **12**: 1–14 (2020).

[23] Madduma-Bandarage U.S.K., Madihally S.V., Synthetic Hydrogels: Synthesis, Novel Trends, and Applications, *J. Appl. Polym. Sci.,* **138**: 1–23 (2021).

[24] Tanan W., Saengsuwan S., Microwave Assisted Synthesis of Poly (acrylamide-co-2-hydroxyethyl methacrylate)/poly(vinyl alcohol) Semi-IPN Hydrogel, *Energy Procedia.*, **56**: 386–393 (2014)

[25] Reowdecha M., Dittanet P., Sae-oui P., Loykulnant S., Prapainainar P., Film and Latex Forms of Silica-Reinforced Natural Rubber Composite Vulcanized Using Electron Beam Irradiation, *Heliyon*., **7**: e07176 (2021)

[26] Zhang C., Easteal A. J., Study of Poly(acrylamide-co-2-acrylamido-2-methylpropane Sulfonic Acid) Hydrogels Made Using Gamma Radiation Initiation, *J. Appl. Polym. Sci.,* **89**:1322–1330 (2003).

[27] Abou El Fadl F. I., Elbarbary A. M., Radiation Synthesis And Characterization of Heterogeneous Magnetic Nanocomposites of 2-Hydroxyethyl Methacrylate for Catalytic Degradation of Sandocryl Blue Dye, *Sep Purif Technol.,* **272**: 118972 (2021).

[28] Micutz M., Lungu R. M., Circu V., Ilis M., Staicu T., Hydrogels obtained via γ-irradiation Based on Poly(Acrylic Acid) And its Copolymers with 2-Hydroxyethyl Methacrylate, *Appl Sci.,* **10**: 4960 (2020).

[29] Eid M., Gamma Radiation Synthesis and Characterization of Starch Based Polyelectrolyte Hydrogels Loaded Silver Nanoparticles, *J. Inorg Organomet Polym Mater.,* **21**: 297–305 (2011)

[30. Budianto E., Muthoharoh S. P., Nizardo N. M., Effect of Crosslinking Agents , pH and Temperature on Swelling Behavior of Cross - linked Chitosan Hydrogel, *Asian J Appl Sci.*, **03**: 2321–893 (2015)

[31] Davaran S., Alimirzalu S., Nejati-Koshki K., Nasrabadi H.T., Akbarzadeh A., Khandaghi A.A., Abbasian M., Alimohammadi S., Physicochemical Characteristics of Fe_3O_4 Magnetic Nanocomposites Based on Poly(N-isopropylacrylamide) for Anti-Cancer Drug Delivery, *Asian Pacific J Cancer Prev.,* **15**:49–54 (2014).

[32] Bayandori Moghaddam A., Hosseini S., Badraghi J., Banaei A., Hybrid Nanocomposite Based on $CoFe_2$ O4 Magnetic Nanoparticles and Polyaniline, *Iran. J. Chem. Chem. Eng. (IJCCE),* **29(4)**:173–179(2010).

[33] Anda-Flores Y.D., Carvajal-Millan E., Campa-Mada A., Lizardi-Mendoza J., Rascon-Chu A., Tanori-CordovaJ., Martínez-López A. L., Polysaccharide-Based Nanoparticles for Colon-Targeted Drug Delivery Systems. *Polysaccharides*., **2(3)**: 626-647 (2021).

[34] Henríquez C. M. G., del Carmen Pizarro Guerra G., Vallejos M.A.S., Rojas de la Fuente S.D., Flores M.T.U., Jimenez L. M. R., In Situ Silver Nanoparticle Formation Embedded into a Photopolymerized Hydrogel with Biocide Properties, *J. Nanostructure Chem.,* **4**: 119–132 (2014).